

FAST LONG RANGE ACTUATOR (FLORA)

Qunyi Chen, Thomas A. Dow, Kenneth Garrard and Alex Sohn
Precision Engineering Center, NC State University
Raleigh, NC

INTRODUCTION

Diamond turning (DT) has revolutionized the fabrication of optical surfaces for consumer, defense and science applications such as contact lenses, forward-looking infrared radar and infrared spectrometers. It has made this impact not only because it can accurately and rapidly fabricate diffractive, refractive and reflective optical surfaces, but also because it can create reference features tied to the optical surfaces to assist in the assembly process. An emerging trend in optical design is the use of Non-Rotational Symmetric (NRS) surfaces to reduce complexity, bulk and weight while improving optical performance. To create these so-called freeform surfaces, DT machines have been operated at very slow spindle speeds or modified with a piezoelectric Fast Tool Servo (FTS) or a flycutter. The proposed Long Range Actuator (FLORA) integrates existing technologies (air bearings, linear motors, high-resolution encoders and real-time control) into a lightweight, moving tool holder that can be retrofitted onto a conventional DT machine.

The goal of the FLORA is to create optical quality surfaces while moving the tool over a range of ± 2 mm at a frequency of 20 Hz. The technical challenges include:

Form Error Diamond turning machines can create excellent form fidelity because of their stiff, linear slides and air-bearing spindles. Reducing the moving mass will improve the bandwidth of the system but also make it more susceptible to disturbances.

Surface Finish Simple theoretical relationships between machining parameters (spindle speed, axis velocity) and tool geometry can be used to predict surface finish. However, the dynamic conditions envisioned for the FLORA may play a more significant role.

SYSTEM DEVELOPMENT

A prototype FLORA was built during 2004 and has continued with support from NSF. The FLORA has a light-weight honeycomb triangular piston, a linear motor and a high-resolution linear encoder. The total range of motion of the motor is 50 mm but the goal is a stroke of 4 mm

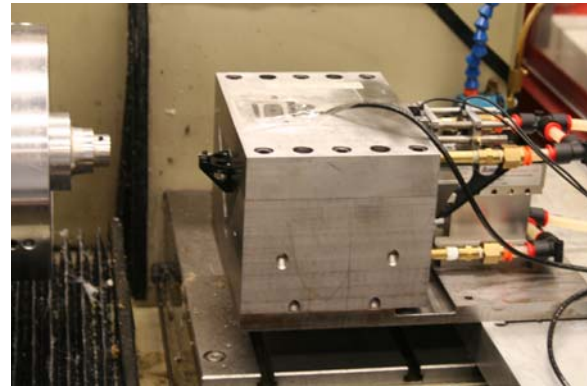


FIGURE 1. Photograph of the FLORA system mounted on the ASG 2500 DTM.

at 20 Hz. A photograph of the actuator is shown in Figure 1.

To improve the surface finish and figure error for this actuator, a number of changes to the electronic components were made over the previous design [1].

High-resolution encoder – A Sony glass scale encoder was added to provide piston position feedback with 0.25 nm resolution at speeds up to 750 mm/sec.

Linear Amplifier – An Aerotech linear amplifier BL10-80A is being used to drive the Airex linear motor. The amplifier has a maximum current output of ± 10 Amps with a bandwidth of 2000 Hz. The motor can produce a peak force of 81 N.

Control platform – A PMDi controller has been installed that can provide an update time of 25 μ sec or 40 Kz. This system uses an Analog Devices SHARC processor 40 MHz ADSP-21061L.

OPEN LOOP TRANSFER FUNCTION

The single DOF system shown in Figure 1 consists of moving piston in an air bearing (an undamped mass m), the actuating force $K_f I$ from the linear motor and the tool feeding position $z(t)$ from the linear encoder. Figure 2(a) shows the measured open loop system transfer function for output in mm to input in current to the amplifier. Figure 2(b) shows the result when the command

amplitude is modified to account for the mass inertia and in this case the transfer function is from mm command to mm motion. The peak in Figure 3(b) at 900 Hz is due to the analog current loop within the amplifier and motor. Additional resonance peaks above 1000 Hz are due to aerodynamic effects in the linear air-bearing.

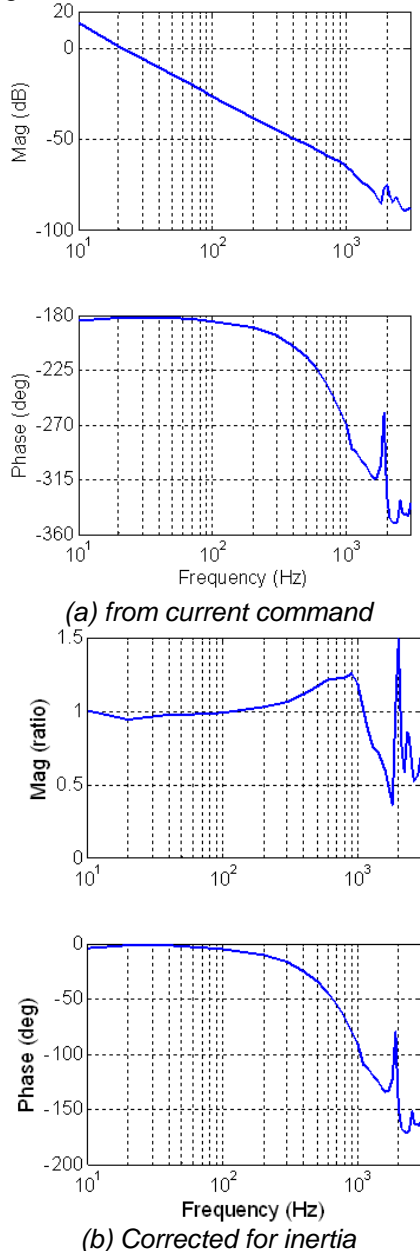


FIGURE 2. Commutated open loop system transfer functions

CONTROL SYSTEM DESIGN AND TESTING

The controller design is based on the measured open loop frequency response and desired

closed-loop system performance specification. A PID controller (Equation (1)) was first designed due to its intuitive nature and the gains are determined by trial-and-error tuning process. A frequency design approach using a lag-lead controller (Equation (2)) was followed to obtain desired frequency response across the desired range of frequencies.

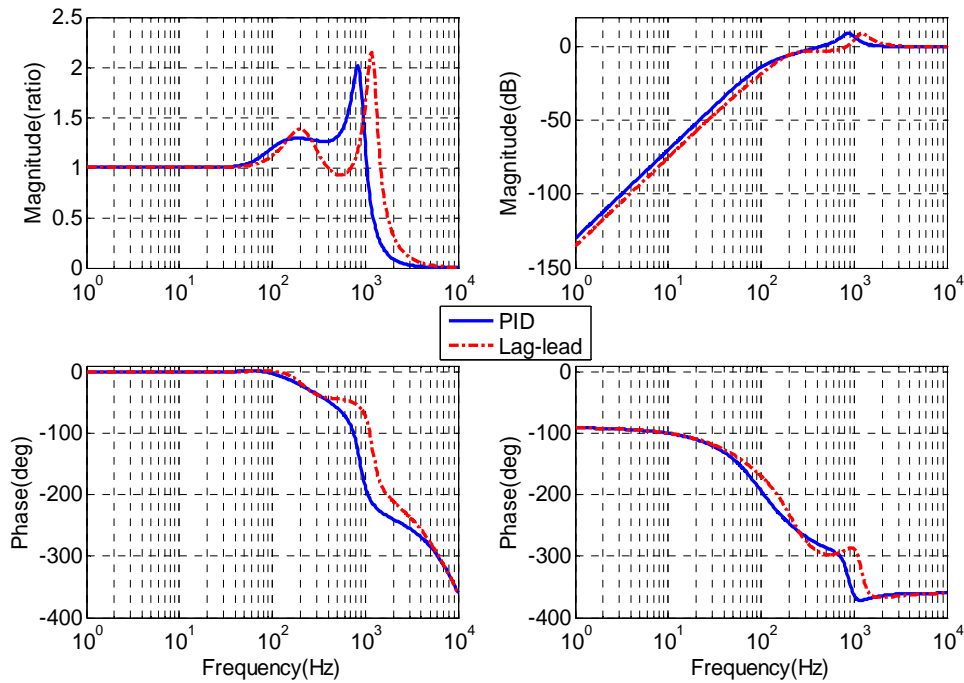
$$K_{PID}(z) = \frac{3321.1z^2 - 6518.9z + 3200}{z^2 - z} \quad (1)$$

$$K_{LL2}(z) = \frac{4355z^3 - 11928z^2 + 10878z - 3303}{2z^3 - 4.4197z^2 + 3.1516z - 0.73186} \quad (2)$$

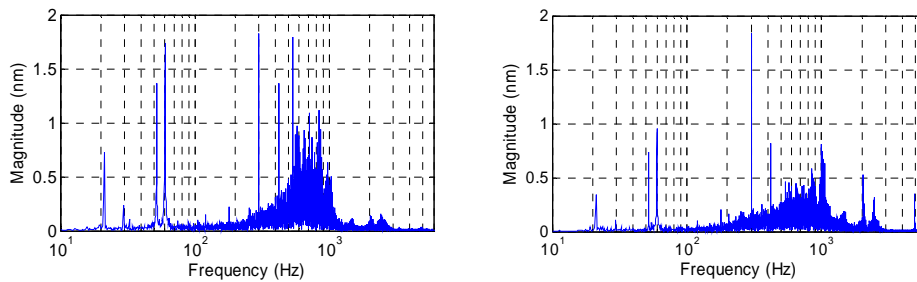
A comparison of the theoretical closed-loop system frequency response is shown in Figure 3. These two controllers behave similarly in the frequency domain; that is, they increase loop gain at low frequency, add phase lead to obtain phase margin at the crossover frequency and lower the gain at high frequency. The transfer function in Figure 3(a) is for position command to the output position. It shows the closed-loop system has a bandwidth of 1122 Hz with the PID controller and 1594 Hz with the lag-lead controller. As a result, the closed-loop response for the lag-lead will be faster but with slightly larger overshoot. The sensitivity function in Figure 3(b) is a measure of the error in tracking commands at low frequencies and rejecting disturbances at high frequencies. The position error is $(1-1/\text{magnitude})$ in this graph and it shows results that would not be visible in Figure 3(a) especially at low frequencies. For a sine wave command using the PID controller at 20 Hz, the magnitude is -52 dB, the error is 0.25% and the amplitude ratio in Figure 3(a) is 0.9975.

It is important to make the sensitivity magnitude small and Figure 3(b) shows the typical trade-offs involved in feedback control design.

1. The lag-lead controller will minimize tracking errors and disturbance forces at frequencies lower than 1000 Hz. Below 100 Hz, the sensitivity magnitude from the lag-lead controller is about half that of the PID controller. Experiments with 60 Hz disturbance have verified this result.
2. Both controllers have nearly the same peak sensitivity magnitude but the lag-lead controller peaks at a higher frequency (1219 Hz) than the PID (875 Hz). This behavior will amplify disturbances above 1000 Hz.



(a) Transfer function (b) Sensitivity function
 FIGURE 3. Closed loop simulations for PID and Lag-lead controllers



(a) PID controller (b) Lag-lead controller
 FIGURE 4. Frequency spectrum of encoder data when holding position

The design process involves a compromise between reducing low frequency error magnitude and improving disturbance rejection at high frequency as shown in Figure 3(b). Figure 4 shows the frequency spectrum of the piston motion when holding position. Error for the PID controller is ± 40 nm PP (10.8 nm RMS) and ± 30 nm PP (8.0 nm RMS) for the Lag-lead. It is clear that the amplitudes are much smaller for frequencies less than 1000 Hz in the case of lag-lead controller.

With these two controllers design, additional studies on sensitivity function have been performed regarding the need for physical damping and most desirable piston mass.

1. Physical damping is not needed for FLORA designs. At high-frequency the amplitude is too small to generate useful forces and at low frequency the damping forces are high but are not needed and only lead to higher motor force.
2. When the magnitude of the sensitivity function exceeds 0 dB, the system relies totally on the mass to reject disturbances. In fact, the controller actually amplifies the disturbances at frequencies higher than crossover frequency (430 Hz for the PID controller and 830 Hz for the lag-lead controller in Figure 3(b)). As a result of the high frequency disturbance with current FLORA design and achievable controller design, the reduction of piston mass will

reduce the system disturbance rejection capability.

CUTTING PERFORMANCE

A flat surface was machined to test the ability of the FLORA piston to hold position while excited by the forces of machining. Figure 1 shows the FLORA mounted on the ASG-2500 DTM. The flat was machined with a 0.5 mm radius diamond tool at 500 rpm with a 2 mm/min feedrate (4 μm/rev) and 2 μm depth of cut on the finish pass. The theoretical finish is 4 nm PP. The Zygo NewView measurement in Figure 5 shows a 144x108 μm patch represents approximately 72 tool passes and has an average surface finish of 9 nm (RMS).

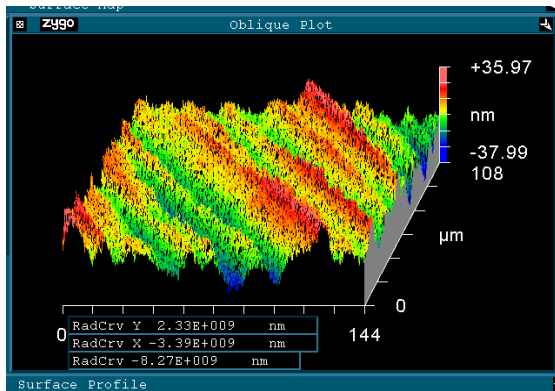


FIGURE 5. ZYGO image of surface finish (RMS=9.0 nm) on a plated copper flat

Table 1 compares the motion of the piston and the RMS finish of flat surface when the tool is locked or held in positioned by the control system. For the locked case, the air pressure was removing from the lower sides of the triangular piston but retaining the preload pressure. This is the same surface finish achieved under these conditions using a standard tool holder. Table 1 shows the piston motion as measured by the encoder. For the locked tool there is little piston motion but when the air bearing is turned on and the motor is used hold the piston, the motion is increased to 8 nm RMS for the Lag-lead controller and 13.1 nm for the PID. The surface finish is also increased when the piston is unlocked. The active closed-loop control using the Lag-lead algorithm adds 2.3 nm RMS to the surface finish and the PID adds 5.6 nm.

TABLE 1. Comparison of RMS error with a locked and position controlled tool holder

	Tool holding method		
	Piston Locked	Lag-lead controller	PID controller
Piston Motion, nm	1	8.0	13.1
RMS Surface finish, nm	6.7	9.0	12.3

CONCLUSIONS

The FLORA control system has been upgraded with a high-resolution encoder, a linear amplifier and a high-speed DSP based controller. The key conclusions are as follows:

1. High controller gain in the frequency range below 1000 Hz is needed to reduce tracking error at 20 Hz and reject cutting force disturbance at the natural frequency of the z slide of the DTM which is approximately 60 Hz. Improved performance could be achieved if the high frequency (>1000 Hz) dynamics within the FLORA can be minimized physically.
2. The feedback control design approach achieved reasonable performance over the range of frequencies of interest. It will be combined with feedforward control and other more advanced control approaches to improve the tool positioning performance.
3. The system changes discussed in this paper improved the position holding capability by 85% over the system described in 2006 [1].

ACKNOWLEDGEMENT

Principal funding for this work is by National Science Foundation grant DMI-0556209, monitored by G. Hazelrigg. PMDi assisted with the development of the control system.

REFERENCES

1) Buescher, N., Dow, T and Sohn, A., "Live Axis Turning", Proceedings of ASPE, Vol 37, 2006, pg 25-28.